

6th Fatigue Design conference, Fatigue Design 2015

Simulation of thermo-mechanical deformation behavior and lifetime of a Nickel-base alloy

Martin Wagner^{a*}, Matthias Decker^a

^aIABG mbH, Einsteinstraße 20, 85521 Ottobrunn, Germany

Abstract

The thermo-mechanical deformation behavior of the Nickel-base alloy 602 CA is simulated by a viscoplastic material model by Chaboche. This model contains elastic properties, nonlinear isotropic and kinematic hardening and time-dependent material behavior. All material parameters for the complex superposition of simultaneously varying mechanical and thermal loadings are identified by isothermal complex low cycle fatigue (CLCF) tests at specific temperatures. These tests contain different strain amplitudes, strain rates and hold times. The parameters are obtained by computational optimization using a deterministic optimization technique (Levenberg-Marquardt algorithm). As a result, thermo-mechanical deformation behavior under various operating conditions can be predicted in terms of the generated stresses. The accuracy of the modeling is verified by corresponding experimental TMF testing. Furthermore, the lifetime of the Nickel-base alloy 602 CA is determined by using a mechanism-based model. The parameters of the model are identified by low cycle fatigue (LCF) tests.

© 2015 Published by Elsevier Ltd. This is an open access article under the CC BY-NC-ND license (<http://creativecommons.org/licenses/by-nc-nd/4.0/>).
Peer-review under responsibility of CETIM

Keywords: Thermo-mechanical fatigue; complex low cycle fatigue; Nickel-base alloy; Chaboche

1. Introduction

Apart from the expansion of renewable energies, fossil energy sources like coal and gas play the largest role in the worldwide electricity generation [1, 2]. The restraint to reduce polluting emissions combined with the optimal utilization of existing resources can only be achieved by increasing the efficiency of gas and steam turbines. For

* Corresponding author. Tel.: +49 89 6088 2847
E-mail address: wagnerm@iabg.de

higher efficiencies it is necessary to raise the gas and steam inlet temperature. This leads to higher mechanical and thermal loadings in combustion chambers and turbine components. In the past, these components were mainly designed due to creep and low cycle fatigue (LCF) loading. Nowadays, there are fluctuations in the current entry to the power supply system by using renewable energies. These fluctuations are balanced by conventional power plants. Start-stop cycles caused by these fluctuations lead to combined thermo-mechanical fatigue (TMF) which is the main damaging factor of the components [1, 3]. For this application Nickel-base alloys are used.

The aim of this work is the simulation of the deformation behavior of the Nickel-base alloy 602 CA under thermo-mechanical loading and the determination of the lifetime. A phenomenological material model provided by Chaboche is used for modeling. The temperature-dependent material parameters are identified by isothermal complex low cycle fatigue (CLCF) tests. Furthermore, the lifetime of the Nickel-base alloy 602 CA is determined for isothermal loading by using a mechanism-based lifetime model, intended as preliminary work for the determination of the lifetime under thermo-mechanical loading in a future step.

2. Material and experimental procedure

In this work the 1220°C solution annealed high temperature resistant Nickel-base alloy 602 CA is used. The chemical composition is shown in Table 1.

Table 1. Chemical composition of Alloy 602 CA.

Element	Ni	Cr	Fe	C	Al	Mn	Ti
Weight-%	basis	25	10	0.2	2	0.5	0.2

TMF tests for characterization of the thermo-mechanical deformation behavior are performed uniaxial under control of the mechanical strain in a servo hydraulic test rig. The specimen geometry is presented in Figure 1.

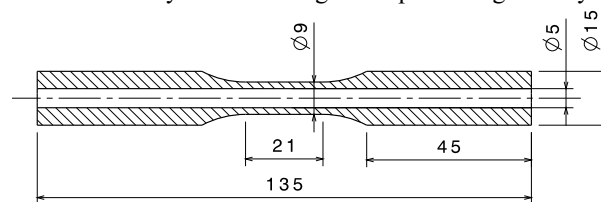


Fig. 1. Specimen geometry.

Five tests are performed in a temperature range between 500 °C und 1000 °C, with mechanical strain amplitudes of $2 \cdot 10^{-3}$, $3 \cdot 10^{-3}$, $4 \cdot 10^{-3}$, $5 \cdot 10^{-3}$ and $6 \cdot 10^{-3}$ and heating and cooling rates of 5 °C/s. Consequently mechanical strain rates of $0.4 \cdot 10^{-4}/s$, $0.6 \cdot 10^{-4}/s$, $0.8 \cdot 10^{-4}/s$, $1.0 \cdot 10^{-4}/s$ and $1.2 \cdot 10^{-4}/s$ are obtained using a triangle shaped signal. The heating of the specimen is conducted by a 5.5 kW high-frequency generator (Hüttinger TIG 5/300). Heat is generated within the material by an induction coil which is fitted to the specimen geometry. Cooling is accomplished by forced air quench of the specimen surface and cooled chuck jaws. A flattened thermocouple (type S) with 0.1 mm thickness is used for temperature measurement [4, 5, 6].

The temperature and mechanical strain input as functions of time as well as the corresponding material response in the form of a stress-strain hysteresis are shown schematically in Figure 2. In this paper out-of-phase (OP) thermo-mechanical fatigue (TMF) tests are carried out which have a phase shift of 180° between the temperature and strain signal. The maximum of mechanical strain occurs at the minimum of temperature. In an OP TMF test a strain ratio of $R_\epsilon = -1$ leads to a positive mean stress considering the temperature dependency of the Young's modulus and the yield stress. Creep effects are observed in compression. The material response is composed of elasticity, isotropic and kinematic hardening as well as the viscosity of the material.

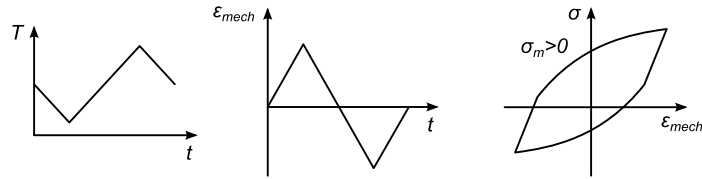


Fig. 2. Temperature input (left) and mechanical strain input (middle) as functions of time, stress-strain hysteresis (right) for an out-of-phase (OP) thermo-mechanical fatigue test (schematic).

3. Modeling

3.1. Material model

A viscoplastic material model with eight parameters provided by Chaboche is used for modeling the thermo-mechanical deformation behavior of the Nickel-base alloy 602 CA [7-9]. The elastic properties of the material are described by Hooke's law, written here in rate formulation,

$$\dot{\sigma} = E \dot{\varepsilon}_{el} = E (\dot{\varepsilon}_{mech} - \dot{\varepsilon}_{pl}) \quad (1)$$

where E is the Young's modulus, σ the stress, ε_{mech} the mechanical strain, ε_{el} the elastic strain and ε_{pl} the plastic strain. The flow function f is used to determine whether a stress state leads to elastic or plastic deformation of the material. It is defined as follows,

$$f = |\sigma - \alpha| - R_e - r \quad (2)$$

where r is the isotropic hardening variable, α the back stress, i.e. the kinematic hardening variable, and R_e the initial yield stress. The material shows an elastic behavior for $f < 0$ and a plastic behavior for $f = 0$. In the case of $f = 0$, the plastic strain rate is calculated as product of the equivalent plastic strain rate and the plastic flow direction $df / d\sigma$. The described relation is defined as flow rule:

$$\dot{\varepsilon}_{pl} = \dot{p} \frac{df}{d\sigma} = \dot{p} \operatorname{sgn}(\sigma - \alpha) \quad (3)$$

The isotropic hardening is described by a linear differential equation of first order:

$$\dot{r} = b(Q_\infty - r) \dot{p} \quad (4)$$

Q_∞ and b are the parameters of isotropic hardening. The isotropic hardening variable r depends exponentially on the equivalent plastic strain p :

$$r = Q_\infty (1 - e^{-bp}) \quad (5)$$

The kinematic hardening is described by the evolution equation by Armstrong and Frederick which is also a linear differential equation of first order:

$$\dot{\alpha} = C_\infty \dot{\varepsilon}_{pl} - \gamma \dot{p} \alpha + \frac{1}{C} \frac{\partial C}{\partial T} \alpha \dot{T} \quad (6)$$

C_∞ and γ are the parameters of kinematic hardening, T is the temperature. The third term in Equation 6 is necessary for calculating the thermo-mechanical deformation behavior. The parameter C is defined as follows:

$$C = \frac{3}{2} C_\infty \gamma \quad (7)$$

The viscosity of the material is described by following equation:

$$\dot{p} = \left\langle \frac{|\sigma - \alpha| - R_e - r}{K} \right\rangle^n \quad (8)$$

This relation is derived by the power law of Chaboche. K and n are the viscosity parameters.

The state variables of the material model are the isotropic hardening variable r and the kinematic hardening variable, i.e. back stress, α . The model parameters are the Young's modulus E , the initial yield stress R_e , the parameters of isotropic hardening Q_∞ and b , the parameters of kinematic hardening C_∞ and γ as well as the viscosity parameters K and n . To simulate the thermo-mechanical deformation behavior it is necessary to calculate the temperature dependence of these parameters.

3.2. Lifetime model

For modeling the lifetime of the Nickel-base alloy 602 CA a mechanism-based model proposed by Seifert and Riedel is used [10,11]. The model was developed for elastic-viscoplastic materials exposed to athermal loading. The relation between the number of cycles to failure N_f and the damage parameter D_{TMF} is illustrated in the following equation:

$$N_f = A(d_n D_{TMF})^{-B} \quad (9)$$

A and B are adjustable parameters. The function d_n depends on the hardening behavior of the material and is a function of the Ramberg-Osgood hardening exponent N_R :

$$d_n = 0,78627 - 3,41692 N_R + 6,11945 N_R^2 - 4,2227 N_R^3 \quad (10)$$

The damage parameter D_{TMF} is defined as follows,

$$D_{TMF} = \frac{Z_D}{\sigma_{cy}} F(t, T) \quad (11)$$

where σ_{cy} is the cyclic yield stress and $F(t, T)$ is a function of the time and temperature history. For isothermal loading $F(t, T) = 1$. The damage parameter Z_D proposed by Heitmann [12] is an estimation for the cyclic J-integral. Z_D is calculated from characteristic quantities of a saturated stress-strain hysteresis loop,

$$Z_D = 1,45 \frac{\Delta\sigma_{eff}^2}{E} + \frac{2,4}{\sqrt{1+3N_R}} \Delta\sigma \Delta\varepsilon_{pl} \quad (12)$$

where E is the Young's modulus, $\Delta\sigma$ and $\Delta\varepsilon_{pl}$ are the stress and plastic strain range of a saturated stress-strain hysteresis loop. Crack closure effects are considered in the effective stress range $\Delta\sigma_{eff}$ containing the stress ratio R of the saturated hysteresis loop:

$$\Delta\sigma_{eff} = \frac{3,72}{(3-R)^{1,74}} |\Delta\sigma| \quad (13)$$

3.3. Parameter identification

In order to identify the parameters of the material model (see Chapter 3.1), a modified low cycle fatigue (LCF) test, a so-called complex low cycle fatigue (CLCF) test, is used [13]. This test is performed uniaxial, isothermal and strain-controlled and contains different mechanical strain amplitudes and strain rates as well as hold times in tension and compression. Therefore it is possible to determine all model parameters at a specific temperature with only one test.

The mechanical strain signal of the CLCF test is presented in Figure 3. During the first seven cycles a mechanical strain amplitude of $4 \cdot 10^{-3}$ is defined. The first five cycles are performed with a mechanical strain rate of $10^{-3}/s$, followed by mechanical strain rates of $10^{-4}/s$ in the sixth cycle and $10^{-5}/s$ in the seventh cycle. Two hold times, each with a duration of 30 minutes, are performed after the seventh cycle. During the first hold time a tensile strain of $4 \cdot 10^{-3}$ is applied and during the second hold time a compressive strain of $-6 \cdot 10^{-3}$ is applied. Subsequent three cycles with a constant mechanical strain amplitude of $6 \cdot 10^{-3}$ and mechanical strain rates of $10^{-3}/s$, $10^{-4}/s$ and $10^{-5}/s$ are performed [6].

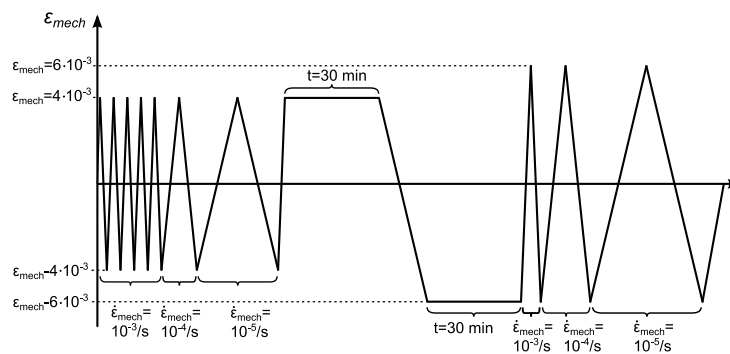


Fig. 3. Mechanical strain input as function of time at a complex low cycle fatigue (CLCF) test.

The corresponding stress response is schematically shown in Figure 4 and shows stress relaxations during the hold times in tension and compression. This phenomenon is well-known as time-dependent material behavior.

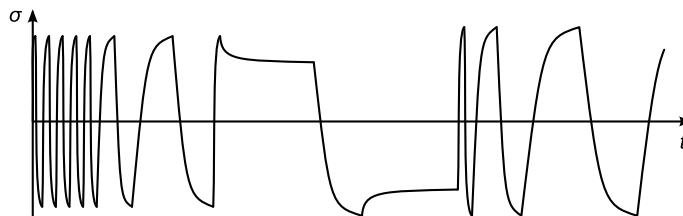


Fig. 4. Stress response as function of time at a complex low cycle fatigue (CLCF) test (schematically), related to the strain signal in Figure 3.

The model parameters are identified by approximation of the model to the engineering stresses which are measured in the CLCF tests. For the optimization of the parameters the gradient-based optimization technique by Levenberg and Marquardt [14] is used. In order to reduce the high influence of hold times and cycles with low strain rate on the optimization, the sum of squares of errors between experimental and calculated stresses,

$$\Phi(E, R_e, Q_\infty, b, C_\infty, \gamma, K, n) = \sum_{i=1}^m [\sigma_i - \sigma(t_i, E, R_e, Q_\infty, b, C_\infty, \gamma, K, n)]^2 \quad (14)$$

is calculated cyclically weighted in each iteration. In detail, the sum of squares of errors of each single cycle and hold time is multiplied by a weighting factor which is inversely proportional to the number of data points. The single sums of squares of errors are accumulated to a total sum of squares of errors [6]. The material equations are solved by the forward Euler integration method [15, 16].

All parameters of the viscoplastic material model depend on the temperature. Therefore the isothermal CLCF tests are performed at the temperatures 500 °C, 600 °C, 700 °C, 800 °C, 900 °C und 1000 °C, according to the temperature range of the TMF tests. Then the parameters are calculated for these temperatures.

For the simulation of the thermo-mechanical deformation behavior all parameters have to be defined in a mathematically closed way as function of temperature. Therefore the parameters are interpolated linear to provide temperature-dependent functions $E(T)$, $R_e(T)$, $Q_\infty(T)$, $b(T)$, $C_\infty(T)$, $\gamma(T)$, $K(T)$ and $n(T)$ for the temperature range between 500 °C und 1000 °C [6].

4. Results

4.1. Parameter identification

The parameters of the material model provided by Chaboche are calculated for the temperatures 500 °C, 600 °C, 700 °C, 800 °C, 900 °C and 1000 °C by the approximation of the calculated stresses to the experimental stresses of each single CLCF test. In Figure 5 the calculated and experimental stresses as material response of the strain signal in Figure 3 are shown for the test temperature of 500 °C [6].

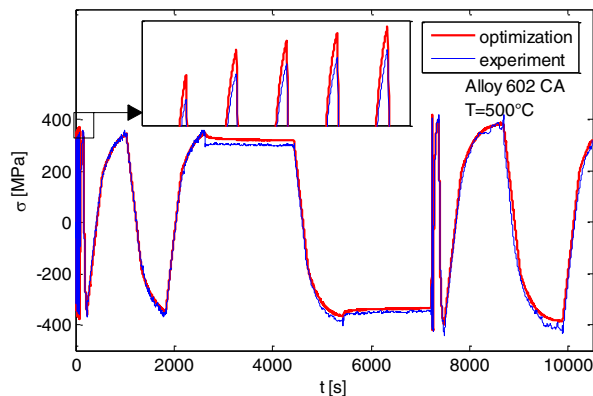


Fig. 5. Calculated and experimental stresses as function of time at the complex low cycle fatigue test (500°C).

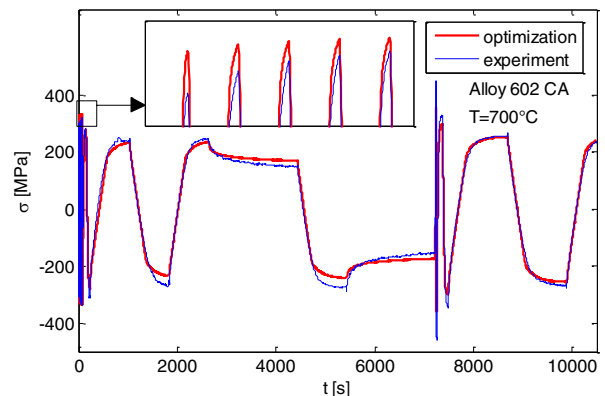


Fig. 6. Calculated and experimental stresses as function of time at the complex low cycle fatigue test (700°C).

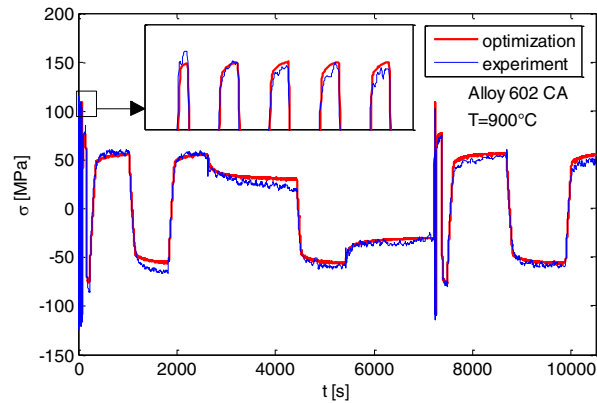


Fig. 7. Calculated and experimental stresses as function of time at the complex low cycle fatigue test (900°C).

The mean deviation between calculated and experimental stresses,

$$\bar{X} = \frac{\sum_{i=1}^m |\sigma_i - \sigma(t_i, E, R_e, Q_\infty, b, C_\infty, \gamma, K, n)|}{\sum_{i=1}^m |\sigma_i|} \cdot 100\% \quad (15)$$

is about 6.5% considering the complete test procedure, i.e. there is a satisfying congruence between test and simulation based on the optimized parameters. The maximum deviation,

$$X_{\max} = \frac{|\sigma_i - \sigma(t_i, E, R_e, Q_\infty, b, C_\infty, \gamma, K, n)|}{|\sigma_i|} \Big|_{\max} \cdot 100\% \quad (16)$$

is about 7.7% and occurs in the fifth cycle. Even though the calculated maximum stresses in the first five cycles are a little too high, cyclic hardening is reproduced quite well by the model. The calculated stress relaxation during the first hold time (35 MPa) is lower than the experimental stress drop (50 MPa). The stress relaxation during the second hold time is reproduced exactly by the material model. Considering the investigations at the temperatures of 600 °C, 700 °C, 800 °C and 900 °C the maximum deviations between test and simulation based on the optimized parameters are a little higher compared with the temperature of 500 °C. Nevertheless, the mean deviations are quite small (about 10%, see Table 2). The low stress level is the reason for the high percental deviations at the temperature of 1000 °C. A better reproduction of the stress relaxation by the model is observed with increasing temperature (see Figure 7) [6].

At the temperatures of 500 °C (see Figure 5), 600 °C and 700 °C (see Figure 6) cyclic hardening is observed during the first five cycles. This cyclic hardening is well reproduced by the model. In contrast, at the temperatures of 800 °C, 900 °C (see Figure 7) and 1000 °C cyclic softening occurs during the first five cycles. At these temperatures the parameters of isotropic hardening Q_∞ and b are optimized to the value of zero so that the calculated stresses show neither cyclic hardening nor cyclic softening.

In Table 2 the maximum and mean deviations between calculated and experimental stresses are presented for all CLCF tests carried out. The investigations at the temperatures of 500 °C, 600 °C, 700 °C, 800 °C and 900 °C show a good reproduction of the experimental stresses by the material model using the optimized parameters [6].

Table 2. Maximum and mean deviations between calculated and experimental stresses (all carried out CLCF tests)

T [°C]	500	600	700	800	900	1000
X _{max} [%]	7.7	16.8	15.7	11.7	14.8	34.3
X̄ [%]	6.5	11.0	8.0	9.8	9.8	30.5

4.2. TMF simulation

Out of phase TMF tests are performed in the temperature range from 500 °C to 1000 °C with different mechanical strain amplitude inputs (see Chapter 2) in order to validate the simulation of the thermo-mechanical deformation behavior. In Figure 8 the second and third cycle of an out of phase TMF test with a mechanical strain amplitude input of $4 \cdot 10^{-3}$ are shown. TMF tests with another mechanical strain amplitudes show qualitative similar results.

During the first cycles there is a good congruence between test and simulation. The maximum deviation in tension and compression is under 10%. The stress relaxation in compression at high temperatures as well as the flattening of the stress-strain hysteresis in tension at low temperatures are exactly reproduced by the model [6].

In Figure 9 the experimental and calculated maximum, mean and minimum stresses of each cycle are presented. The positive mean stress due to out of phase loading is well reproduced by the material model. The TMF test shows cyclic softening in tension and compression. However, the model is not able to reproduce this cyclic softening using the values of the parameters of isotropic hardening Q_∞ and b calculated by approximation to CLCF tests at the temperatures of 800 °C, 900 °C and 1000 °C. Therefore the values of the isotropic hardening parameters are manually fixed to $Q_\infty(800^\circ\text{C})=-100 \text{ MPa}$, $Q_\infty(900^\circ\text{C})=-115 \text{ MPa}$, $Q_\infty(1000^\circ\text{C})=-120 \text{ MPa}$, $b(800^\circ\text{C})=10$, $b(900^\circ\text{C})=11$, $b(1000^\circ\text{C})=12$ for demonstration in Figure 9. Additionally, the used material model does not contain a damage model. Hence, the decrease of stresses caused by crack initiation and propagation is not modelled. Therefore TMF test and simulation are illustrated up to the 300th cycle only (see Figure 9) [6].

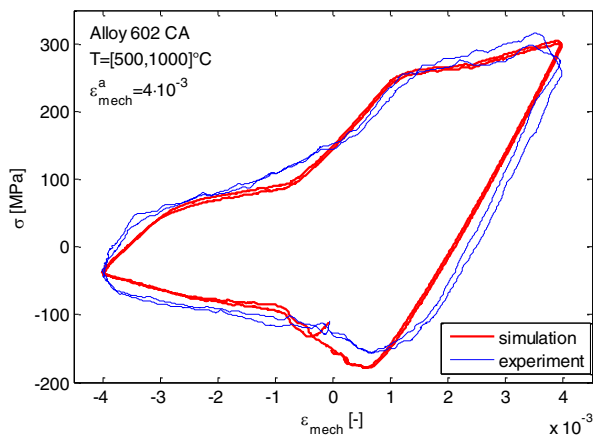


Fig. 8. Stress-strain hysteresis loops for the OP TMF test with a mechanical strain amplitude input of $4 \cdot 10^{-3}$ (second and third cycle) - comparison of calculated and experimental stresses.

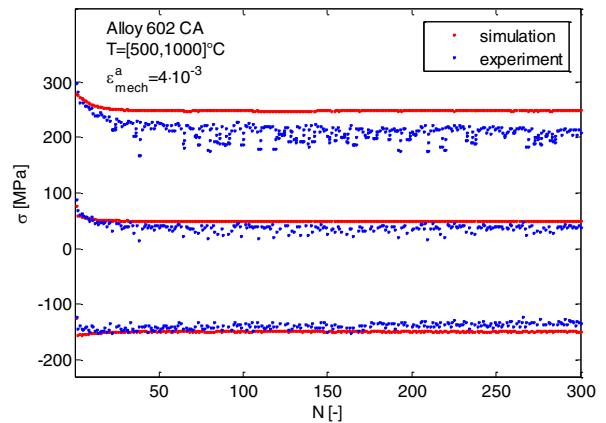


Fig. 9. Cyclic hardening/ softening curve for the OP TMF test with a mechanical strain amplitude input of $4 \cdot 10^{-3}$ – comparison of calculated (parameters of isotropic hardening manual adjusted) and experimental stresses.

4.3. Lifetime investigations

Subsequent to the complex low cycle fatigue (CLCF) procedure (see Chapter 3.3) the specimens are cyclically exposed to isothermal low cycle fatigue (LCF) loading until failure. LCF loading is performed with a constant mechanical strain amplitude of $6 \cdot 10^{-3}$, a constant mechanical strain rate of $2 \cdot 10^{-3}/s$ and a strain ratio of $R_\epsilon = -1$. Thus, six preloaded isothermal tests from 500 °C to 1000 °C are available for lifetime modeling. Additionally, one LCF test without preloading is performed at a temperature of 500 °C. In Figure 10 the saturated stress-strain hysteresis loops, i.e. at half number of cycles to failure $N_f/2$, are presented for all performed tests.

The damage parameter Z_D is calculated using the stress range $\Delta\sigma$ and the plastic strain range $\Delta\epsilon_{pl}$ of these saturated hysteresis loops (see Equation 12). The function d_n and the damage parameter D_{TMF} are calculated by Equations 10 and 11. As mentioned in Chapter 3.2 the function $F(t, T)$ has the value of one for isothermal loading. In Figure 11 the calculated values of the product $d_n D_{TMF}$ are presented as function of the experimental number of cycles to failure N_f for all performed tests. Additionally the calculated damage Wöhler curve is plotted (continuous black line). The values for the adjustable parameters $A = 1.85 \cdot 10^{-5}$ and $B = 3.55$ are calculated by regression analysis (see Equation 9). All performed tests lie within a scatter band of factor 2 around the model curve represented by the dashed lines in Figure 11. Therefore the mechanism-based model is suitable to calculate the lifetime of the Nickel-base alloy 602 CA caused by isothermal loading.

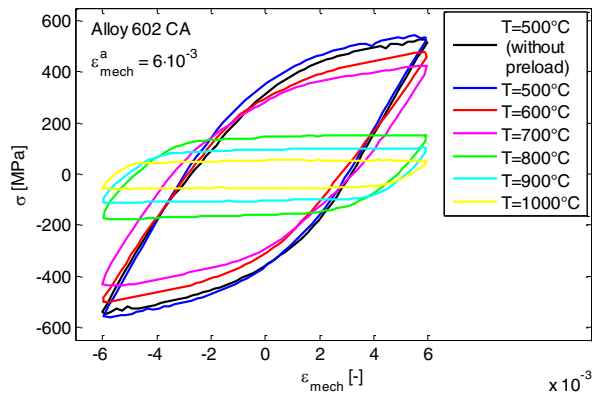


Fig. 10. Saturated stress-strain hysteresis loops, i.e. at half number of cycles to failure $N_f/2$ for all isothermal tests (mechanical strain amplitude input of $6 \cdot 10^{-3}$).

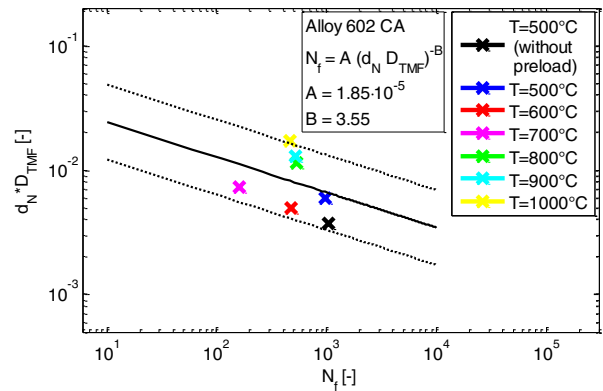


Fig. 11. Values of $d_n D_{TMF}$ as function of the experimental number of cycles to failure N_f for all performed tests, calculated damage Wöhler curve (continuous black line) and a scatter band of factor 2 (dashed lines).

5. Summary and conclusions

The aim of this work was to model the deformation behavior of the Nickel-base alloy 602 CA under thermo-mechanical loading in the temperature range between 500 °C and 1000 °C with an eight-parameter material model provided by Chaboche. The model considers the material mechanisms of elasticity, isotropic and kinematic hardening as well as viscosity. Isothermal complex low cycle fatigue (CLCF) tests were performed at specific temperatures in the temperature range between 500 °C and 1000 °C to identify the model parameters. The parameters were identified by approximation of the model to CLCF test data using the Levenberg-Marquardt algorithm. The thermo-mechanical deformation behavior was simulated using the calculated temperature-dependent parameters. The simulation was performed with test parameters (i.e. temperature range, mechanical strain amplitude and mechanical strain rate) lying inside the test parameters of the CLCF tests which were used to identify the material parameters. Additionally the suitability of a mechanism-based model provided by Seifert and Riedel was checked to describe the lifetime of Alloy 602 CA under isothermal loading. The damage parameter D_{TMF} was

calculated by evaluating saturated stress-strain hysteresis loops and the adjustable parameters A and B of the model were identified by regression analysis.

The approximation of the CLCF tests by the material model shows good results for the temperatures from 500 °C to 900 °C (maximum mean deviation of 11%). The approximation of the CLCF test at a temperature of 1000 °C shows higher deviations because of the lower stress level. Consequently there is a good congruence between TMF test and TMF simulation during the first cycles (<10% deviation).

The cyclic hardening during the first five cycles of the CLCF tests at 500 °C, 600 °C and 700 °C is well reproduced by the material model. Though, the model is not able to reproduce the cyclic softening at 800 °C, 900 °C and 1000 °C. Hence, the cyclic softening appearing in tension and compression of the TMF tests is not determined by the simulation. It is possible to reproduce cyclic softening in TMF and CLCF tests by adjusting the parameters of isotropic hardening Q_∞ and b to negative values within the temperature range from 800 °C to 1000 °C. The disadvantage of this procedure is the increase of the mean deviation between CLCF test and simulation based on the optimized parameters.

The mechanism-based model used for lifetime prediction is suitable for the application with Alloy 602 CA under isothermal cyclic loading. Though, a little number of tests was used for the evaluation of the lifetime, as well as the cyclic loading was performed after CLCF preloading, all tests lie within a scatter band of factor 2 and therefore show a good result. In a future step the mechanism-based model will be used for the determination of the lifetime under thermo-mechanical loading by using TMF results and including the time and temperature-dependent function $F(t,T)$ into the model.

References

- [1] G. Maier, Mikrostruktur, Verformung und Lebensdauer der Legierung Alloy 617B - Experimente, Modelle und Bauteilvorhersagen, Ph.D. Thesis, Karlsruher Institut für Technologie KIT, 2013.
- [2] U.S. Energy Information Administration EIA, International Energy Outlook 2011, DOE/EIA-0484, 2011.
- [3] H.-J. Christ, V. Bauer, Adapting a multi-component model to cyclic stress-strain behaviour under thermomechanical fatigue conditions, Computational Materials Science 57 (2012) 59-66.
- [4] F. Wilhelm, J. Spachtholz, M. Wagner, C. Kliemt, J. Hammer, Simulation of the Viscoplastic Material Behaviour of Cast Aluminium Alloys due to Thermal-Mechanical Loading, Journal of Materials Science and Engineering A 4 (1) (2014) 56-64.
- [5] P. Heuler, R. Heidenreich, Schwingfestigkeitsprüfung von Werkstoffen bei erhöhten Temperaturen - Teil 1: Prüftechnik, Probenformen, Versuchsdurchführung, Datenerfassung, Materialprüfung 34 (1992) 23-28.
- [6] M. Wagner, F. Wilhelm, C. Kliemt, Simulation des viskoplastischen Verformungsverhaltens einer Nickelbasislegierung mit einem kontinuumsmechanischen Materialmodell, Langzeitverhalten warmfester Stähle und Hochtemperaturwerkstoffe, 2014.
- [7] J. Lemaitre, J.-L. Chaboche, Mechanics of solid materials, Cambridge University Press, 1990.
- [8] J.-L. Chaboche, A review of some plasticity and viscoplasticity constitutive theories, International Journal of Plasticity 24 (2008) 1642-1693.
- [9] J. Tong, Z.-L. Zhan, B. Vermeulen, Modelling of cyclic plasticity and viscoplasticity of a nickel-based alloy using Chaboche constitutive equations, International Journal of Fatigue 26 (2004) 829-837.
- [10] T. Seifert, H. Riedel, Mechanism-based thermomechanical fatigue life prediction of cast iron. Part I: Models, International Journal of Fatigue 32 (2010) 1358–1367.
- [11] T. Seifert, G. Maier, A. Uihlein, K.-H. Lang, H. Riedel, Mechanism-based thermomechanical fatigue life prediction of cast iron. Part II: Comparison of model prediction with experiments, International Journal of Fatigue 32 (2010) 1368–1377.
- [12] H. H. Heitmann, H. Vehoff, P. Neumann, Life prediction for random load fatigue based on the growth behavior of microcracks, Advances in Fracture Research 84 - proceedings of ICF6, vol. 5, Oxford/New York, Pergamon Press Ltd., 1984.
- [13] T. Seifert, Ein komplexes LCF-Versuchsprogramm zur schnellen und günstigen Werkstoffparameteridentifizierung, Tagung Werkstoffprüfung, 2006.
- [14] K. Levenberg, A method for the solution of certain problems in least squares, Quarterly of Applied Mathematics 2 (1944) 164-168.
- [15] J.C. Simo, T.J.R. Hughes, Computational Inelasticity, Springer, 1998.
- [16] F. Dunne, N. Petrinic, Introduction to Computational Plasticity, Oxford University Press, 2004.